Proceedings World Geothermal Congress 2015
Melbourne, Australia, 19-25 April 2015

Curie Point Depth Map For Western Afghanistan Deduced From The Analysis Of Aeromagnetic Data

H. Saibi[1], E. Aboud[2,3] and M. Azizi[1]

[1]Department of Earth Resources Engineering, Faculty of Engineering, Kyushu University, Fukuoka, Japan

saibi-hakim@mine.kyushu-u.ac.jp

[2]Geohazards Research center (GRC), King Abdulaziz University, Jeddah, Saudi Arabia

[3]National Research Institute of Astronomy and Geophysics, Cairo, Egypt

Keywords: Geothermal gradient, heat flow, hot spring, aeromagnetic, Curie-point depth (CPD), Afghanistan

ABSTRACT

The geologic setting of Afghanistan has the potential to contain natural resources such as minerals and petroleum as well as geothermal resources. Although, much of the country's potential remains unknown due to lack in exploration. In that regard, a joint project has been formed between USGS and Afghanistan Geological Survey (AGS) to implement aeromagnetic survey over the country. In the present work, aeromagnetic data will be used to estimate the Curie Point Depth (CPD) in order to evaluate the geothermal resources within the country.

CPD is an isothermal surface at which magnetic minerals lose their magnetization (580 °C). In order to achieve this goal, the spectral analysis technique will be used for the aeromagnetic data to estimate the CPD and link it to geothermal activity in Afghanistan where there are four well known geothermal fields spreading out in the western portion of the country.

The results show that there are four regions which can be characterized by CPD: 1) Shallow curie depths (~16 – 21 km) are located at Helmand basin. 2) Intermediate curie depths (~21 – 27 km) are located at south of Helmand basin (Baluchistan geothermal field associated with carbonatitic post-volcanic processes) and southeast of Helmand basin (Helmand-Arghandab geothermal field associated with Arghandab granitoid massifs). 3) Deep curie depths (~25 – 35 km) are located at Farad block (Farahrud geothermal field associated with Pasavand deep-seated fault and fracture system) and Helmand block. 4) Very deep curie depths (~35 – 40 km) are located at the western part of the north Afghanistan platform along the Herat fault system.

Our results imply a geothermal gradient ranging from 14.50 °C/km to 36.25 °C/km and heat-flow values ranging from 36.25 to 90 mW/m^2 for the study area. The hot springs discharge mainly along deep-seated major faults bordering the tectonic blocks in Afghanistan. The deduced thermal structure in western Afghanistan has a relationship with the collision of the continental Indian and Eurasian plates. The shallow CPDs values are related to the Kandahar arc.

1. INTRODUCTION

To study the thermal structure inside the Earth, geoscientists use mainly two methods: direct and indirect methods: The direct method consists of direct measurement performed in boreholes (from few meters to several kilometers in depth) which is not available globally, and indirect methods are based on geophysical data analysis. The indirect methods have several constraints and limitations such as depth resolution, which depends on the survey dimension, and complexity of geological structures that can cause significant errors in estimation of Curie Point Depth (CPD) (Okubo and Matsunaga, 1994).

In this study, the spectral analysis technique will be utilized in order to estimate the CPD from aeromagnetic data over the western portion of Afghanistan. Laboratory experiments showed that ferromagnetic materials lose their magnetism above the Curie temperature (580 °C) because the thermal energy is sufficient to maintain a random alignment of the magnetic moments of the iron minerals (Hinze et al., 2013). Therefore, an estimate of the bottom of magnetized crust represents a direct indicator of the Curie isotherm, and variations in the thickness of the magnetized crust can be explained as variations in temperature (Manea and Manea, 2011).

The objectives of this paper are to estimate the CPD using a spectral analysis applied to aeromagnetic anomalies, and to provide geothermal gradient and heat flow maps for western Afghanistan. The results will be helpful for future geothermal developments in this country.

Estimations of the CPD began in the 19th century where researchers used this criteria for geothermal exploration. For example: Bhattacharyya and Leu (1975) analyzed the magnetic anomalies over Yellowstone National Park and mapped the CPD for geothermal reconnaissance. Wasilewski et al. (1979) mentioned that the Moho surface is a magnetic boundary and related with CPD. Okubo et al. (1985) estimated the CPD of Kyushu Island (Japan) from aeromagnetic data and compared them with volcanic localities. Blakely (1988) mapped the CPD using aeromagnetic data in Nevada. Tanaka et al. (1999) mapped the CPD in East and Southeast Asia. Ruiz and Introcaso (2004) mapped the CPD in western Argentina. Chiozzi et al. (2005) mapped the CPD in Central-southern Europe. Aydin et al. (2005) mapped the CPD of Turkey. Tanaka and Ishikawa (2005) mapped the CPD in Japan. Ross et al. (2006) mapped the CPD in California. Espinosa-Cardeña and Campos-Enriquez (2008) determined the CPD, geothermal gradient, and heat flow of Cerro Prieto geothermal field in Baja California (Mexico) using spectral analysis of aeromagnetic data. Rajaram et al. (2009) mapped the CPD of Indian subcontinent. Bouligand et al. (2009) mapped the CPD of Western United States using a fractal model for crustal magnetization. Ebbing et al. (2009) mapped the CPD in mid-Norwegian margin. Rozimant et al.

(2009) mapped the CPD in Slovakia. Manea and Manea (2011) estimated the CPD in Mexico. Aboud et al. (2011) mapped the CPD of Sinai Peninsula (Egypt). Kharastathis et al. (2011) investigated the structure of the geothermal field of the North Euboean Gulf in Greece. De Ritis et al. (2013) detected shallow heat source in the central Aeolian Ridge (Italy) from CPD analysis using aeromagnetic data. Guimarães et al. (2014) mapped the CPD in Central Brazil. Hsieh et al. (2014) mapped the CPD in Taiwan. Salem et al. (2014) mapped the CPD across the central Red Sea.

In our study, we estimated the CPD from the aeromagnetic data at the western portion of the country and the results showed that shallow (16 km) and very deep (40 Km) CPD were detected in the study area having a direct relation to the tectonic and geothermal activity in the study area. More details will be discussed within their context.

2. GEOLOGICAL AND TECTONIC SETTINGS

A geomorphologically color shaded relief map of Afghanistan and the surrounding area (Figure 1) shows the large area of mountainous terrain in the country, especially in the central and northeastern parts compared with the relative lowlands to the southwest. Furthermore, the mountain belt is not linear. This tectonic morphology is a direct result of the India-Asia collision to the east of Afghanistan.

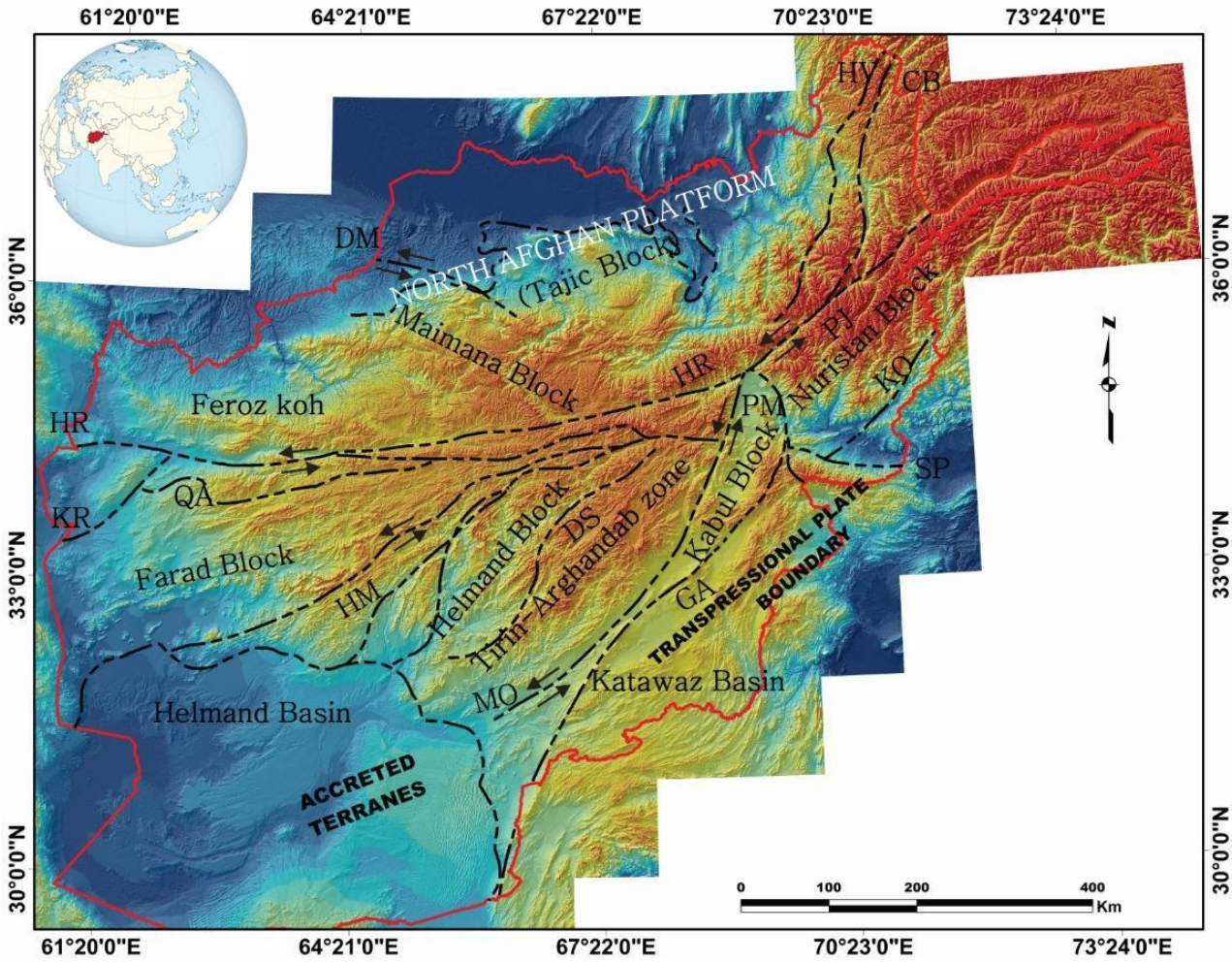

Figure 1: Color shaded relief map of Afghanistan topography including tectonic block names and abbreviations of major faults. CH, Chaman; CB, Central Badakhsan; DS, Darafshan; DM, Dosi Mirzavalan; GA, Gardez; HR, Hari Rod; HM, Helmand; HV, Henjvan; KR, Kaj Rod; KO, Konar; MO, Mokur; PM, Paghman; PJ, Panjshir; QA, Qarghanaw; SP, Spinghar.

Afghanistan has some of the most complex and varied geology in the world. The oldest rocks are of Archean age and are succeeded by rocks from the Proterozoic and from all of the Phanerozoic system up to the present day (Figure 2). The country also has a long and complicated tectonic history, partly related to its position at the western end of the Himalaya.

The tectonic evolution of Afghanistan from Late Palaeozoic times onwards is best explained in terms of accretion of fragments of Gondwana to the active margin of Laurasia from late Palaeozoic times onwards (Tapponnier et al., 1981). During the Triassic, parts of the northern edge of the Gondwanaland supercontinent broke away and began drifting north, before colliding with the Tajic block, resulting in the Cimmeride Orogeny. The orogeny is marked by two distinct collisions, which brought first the Farad block against the Tajic block, followed closely by the Helmand block against the Farad block. The Herat fault system marks the suture line of this first collision, which had taken place and was completed by the beginning of the Cretaceous, and the Panjao Suture marks the line of the second collision that was completed by early Cretaceous times. Both suture zones are ophiolite bearing, and the Herat Fault system in particular has had a long history of sedimentation and igneous activity, up to the present. The Farad block was subsequently overlain by Upper Jurassic-Cretaceous sediments and the Helmand block by Cretaceous sediments only. During

this period the Pamir and West Nuristan blocks of northeast Afghanistan were also accreted to Eurasia. These four blocks, together with the Tajic block are collectively known as the Afghan Block. Due to processes discussed below, the southeastern margin of this Block is considered prospective for precious and base metal mineralisation, as well as rare metals in the numerous pegmatite fields.

Following a brief period of quiescence, tectonic activity once again began as India drifted north, away from Gondwanaland and towards the enlarged Eurasian plate with the Afghan block at its southern margin. The first evidence of this is preserved as the Kandahar volcanics, which marked the beginning of the development of a volcanic arc along the southern margins of the Eurasian plate. These were intruded by subduction-related, 'I-type' granitoids in the Helmand and West Nuristan blocks (during the Cretaceous to early Tertiary). This geological setting is highly prospective for a number of different mineralisation styles and the large number of mineral discoveries to date only reinforces the potential of the East-Central Afghanistan region. Igneous activity was not confined to this region, with younger (Oligocene) alkaline intrusions and basaltic extrusions in the Farad block and the sedimentary basins within the Herat fault zone. The chemistry of these rocks suggests derivation from a mantle source beneath a zone of continental extension (within an overall setting of dextral transtension). Oligocene granitoids were also intruded into the thickened continental crust of Northeast Afghanistan. By the start of the Tertiary, the widespread marine sedimentation that had preceded the Himalayan Orogeny had become restricted to the Tajic block and by Neogene times even this had become localised as the collision of India began to raise the area above sea level. Himalayan deformation of the Afghan block resulted in the reactivation of many of the internal block boundaries including the Herat fault system (as discussed above, but not active since the Miocene) and the Chaman Fault system (which marks the southeast edge of the Afghan Block and is still active to the present day). Folding and thrusting of the Mesozoic sediments also led to basin inversion and imbrication with the Palaeozoic basement.

To the east of the Afghan block a complex collage of tectonic units marks the collision zone with the Indian plate. During the Cretaceous period, the East Nuristan volcanic arc was accreted to the margin of Eurasia (although magmatism continued in the Eocene). This was followed by the docking of the Kabul block. The Kabul block is somewhat of an enigma in Afghan geology. It is composed of Proterozoic and Lower Palaeozoic basement overlain by Mesozoic sedimentary sequences, and is bounded along its western and eastern margins by ophiolitic rocks of Cretaceous age. It is believed that the block was a sliver of continental crust, separated from the Indian and Afghan blocks by oceanic crust, which got caught up in the collision and was accreted to the edge of the Afghan Block before final collision with India. The Kabul block is particularly prospective for stratiform copper deposits hosted in Vendian – Cambrian metasedimentary rocks, and for chromite in the ophiolitic sequences. The final piece in the Afghanisan jigsaw is the Katawaz basin in Southeast Afghanistan. This is interpreted as a flexural basin on the western margin of the Indian Plate, where subsidence synchronous with sedimentation resulted in the deposition of more than 10 km of Tertiary sediments before shortening and inversion in the late Tertiary as India finally collided with Afghanistan. Sedimentation across the country since this time has been continental in nature, with large areas of Quaternary deposits particularly across the very north and south of the country.

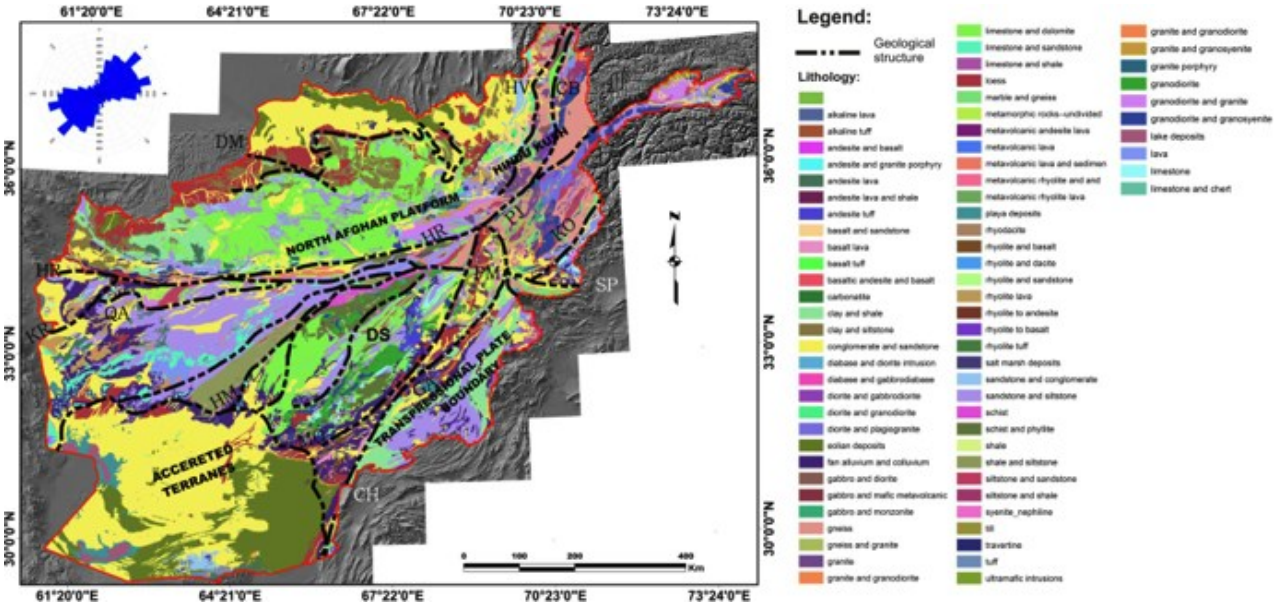

Figure 2: Geological map showing rock units in Afghanistan and the locations of major faults (modified from Mihalasky et al., 2007), overlaid on the shaded relief (SRTM) map. Rose diagram shows the direction of the geological faults, striking mainly in NE-SW and ENE-WSW directions.

3. GEOTHERMAL SETTINGS

The geothermal potentialities of Afghanistan are still unknown. Just a few initial-stage geothermal exploration projects have been started in 1969 with no drilling programs and no advanced technologies for real geothermal reservoir characterizations. Afghanistan is created by the collision of the Indian and Eurasian plates along the Herat-Panjshir E-W geosuture (deep seated strike-slip fault), resulting in the uplifting of the Hindu-Kush on this axis (65 Ma.), so many geothermal manifestations are present especially along the neotectonic regions generated from these collisions and associated with the Paleo-Neo-Quaternary volcanism. In many cases, the thermal indicators are close to recent young fractured granitic massifs. The volcanic rocks are widespread in the central and southwestern parts of Afghanistan (Shareq et al., 1980) and many magmatic intrusive rocks are present in many places of the country with 8% of the country's total surface area (Musazai, 1994).

Geothermal energy in Afghanistan has been used mainly for medical purposes and other applications such as food processing, carpet and wood processing, greenhouse, and small-scale industries.

Geopressured reservoirs were recorded in the oil and gas fields of the northern parts of Afghanistan (Kurenoe and Belianin, 1969). These high-pressured geothermal reservoirs are located in deeper parts (3 to 8 km deep) with fossil waters (Saba et al., 2004).

The geothermal fields in Afghanistan are mainly water-dominated systems (Saba et al., 2004). The main controlling factors in the formation of the thermal water systems is the neotectonic activity in the region, which facilitates the creation of paths for waters to flow through faults. The hydrothermal systems are associated with the major faults that divide Afghanistan into many structural blocks. The four main geothermal fields located in Afghanistan are: the Harirud-Badakhshan, the Helmand-Arghandab, the Farahrud, and the Baluchistan geothermal fields.

3.1 The Harirud-Badakhshan Geothermal Field (HBGF)

This geothermal field extends throughout the length of the geosuture structural zone of central Afghanistan. It extends from Heart in western Afghanistan up to Pamirs to the northeastern boundary of the country. In the western part, the hot springs are nitrogen-bearing siliceous with a discharge surface temperature ranging from 48 to 52 ˚C. In the central part, the hot springs have surface temperatures of 24-35 ˚C and are rich in chemical concentrations (TDS up to 3g/L) with high amount of CO_2 due to the metamorphic environments. In the western part, the hot springs have lower geochemical concentrations compared to westerly counterparts and contain some amounts of hydrogen sulfide in their solutions (Saba et al., 2004).

3.2 Helmand-Arghandab Geothermal Field (HAGF)

This geothermal field is characterized by CO_2-nitrogen-bearing thermal waters. The hydrogeothermal activities are associated with the Helmand-Arghandab granitoid massifs. The deep-seated Chaman-Mokur (CH-MO in Figure 1) fault system, and other groups of secondary faults are the main structural factors in the formation of this geothermal field, which covers regions such as Helmand, Mokur, and Tirin-Azhdar in south-central of Afghanistan. The geothermal manifestations are in the vicinities of the CH-MO fault system, rich in alkali and rare earth elements (Saba et al., 2004).

3.3 The Farahrud Geothermal Field (FGF)

This geothermal field is located in the Farahrud structural depression in southwestern Afghanistan. Geothermal activity in the form of hydrothermal springs in this field is associated with Pasaband deep-seated fault and fracture system. The hot waters are rich in bicarbonate, calcium, and silica (Saba et al., 2004).

3.4 The Baluchistan Geothermal Field (BGF)

To the extreme southwestern corner of Afghanistan lies the volcanic terrain of Chagai-e in Baluchistan, with lots of hydrothermal activity. These hydrothermal activities are suggested to be associated with carbonatitic post-volcanic processes in this region, resulting in the deposits of beautiful onyx marbles. The hydrothermal activity, mainly of brine nature, is rich in CO_2, calcium, and chloride (Saba et al., 2004).

4. AEROMAGNETIC ANOMALIES

The magnetic dataset is derived from the 2006 and 2008 aeromagnetic surveys provided by U.S. Geological Survey and the Naval Research Laboratory (NRL) (Ashan et al., 2007; Shenwary et al., 2011). The grid elevation is 5,000 m above terrain. Five base station magnetometers were used during the survey. In order to correct the airborne magnetic data for time-varying anomalies, a weighted average of data from the five base stations was used to predict the time-varying field at the aircraft. To overcome bi-polarity related problems, the total magnetic intensity data are gridded by minimum curvated method (with a grid size of 1000 m) and then reduced to the pole (RTP) using magnetic inclination of 48.74° and a declination of 2.01°. Magnetic data ranges from -168 nT to 650 nT (Figure 3).

4.1 The central region

This area starts from Kandahar to the northwest up to central Afghan swell. It includes two sedimentary basins (Ghor basin and Rosgan basin) and two swell regions (Central Afghan swell and Sharistan swell). The thickness of sedimentary formations in Ghor basin is 10 km and is 2 km in Rosgan basin (Bosum et al., 1968).

The RTP magnetic map shows clearly the two basins with low anomalies. The Sharistan swell, located between the two basins is represented by medium anomalies (around 25 nT) striking NE-SW similar to that of “Kandahar Swell”. This region has many dike intrusions. High magnetic anomalies are along the Helmand fault (HM) and show the extension of such anomalies in the accreted terranes in the western part of Afghanistan. The magnetic anomalies in the Sharistan Swell have a good correlation with the location of dykes and Archean rocks. To the northwest the anomalies decrease at Ghor basin, which reflects the subsidence of the magnetic crystalline basement in this area. Some isolated anomalies in the Ghor basin exist and could be explained by the location of acid magnetic rock intrusions.

The magnetic anomalies in the Ghor and Rosgan basins differ from one another because of the depths of the magnetic crystalline rocks. We notice high magnetic anomalies in Central Afghan swell reaching 170 nT. The anomalies are parallel to HR fault, striking E-W direction.

4.2 The western regions

The magnetic anomalies of the western regions show an entirely different picture than those of the eastern regions. The local anomalies in the south are similar to those of Kandahar region as they have both ophiolites rocks.

4.2.1 Hilmand depression

It is located in the southwestern part of the survey area and consists of large deserts. This area has not been geologically explored compared to other parts of south Afghanistan due to its inaccessibility. The Hilmand depression consists of Neogene and Quaternary sediments. This region shows many high-distributed magnetic anomalies (ranging from 145 nT to 280 nT). The interpretation of such anomalies is that this region might contain an old block of crystalline rocks covered by thin sedimentary layers.

4.2.2 Anomaly of Chakansur

This region has a very strong magnetic anomaly (190 nT to 650 nT in the north). The source of the high magnetism in this area could be the existence of strong magnetic intrusion body underground (may be gabbro).

4.2.3 Farah region

In this region, a predominant magnetic anomaly (around 180 nT) striking mainly in E-W direction extends more than 200 km along the Farah fault. This region has Tertiary volcanic rocks including granites, which may cause these anomalies and possible upwarping of the magnetic basement is considered.

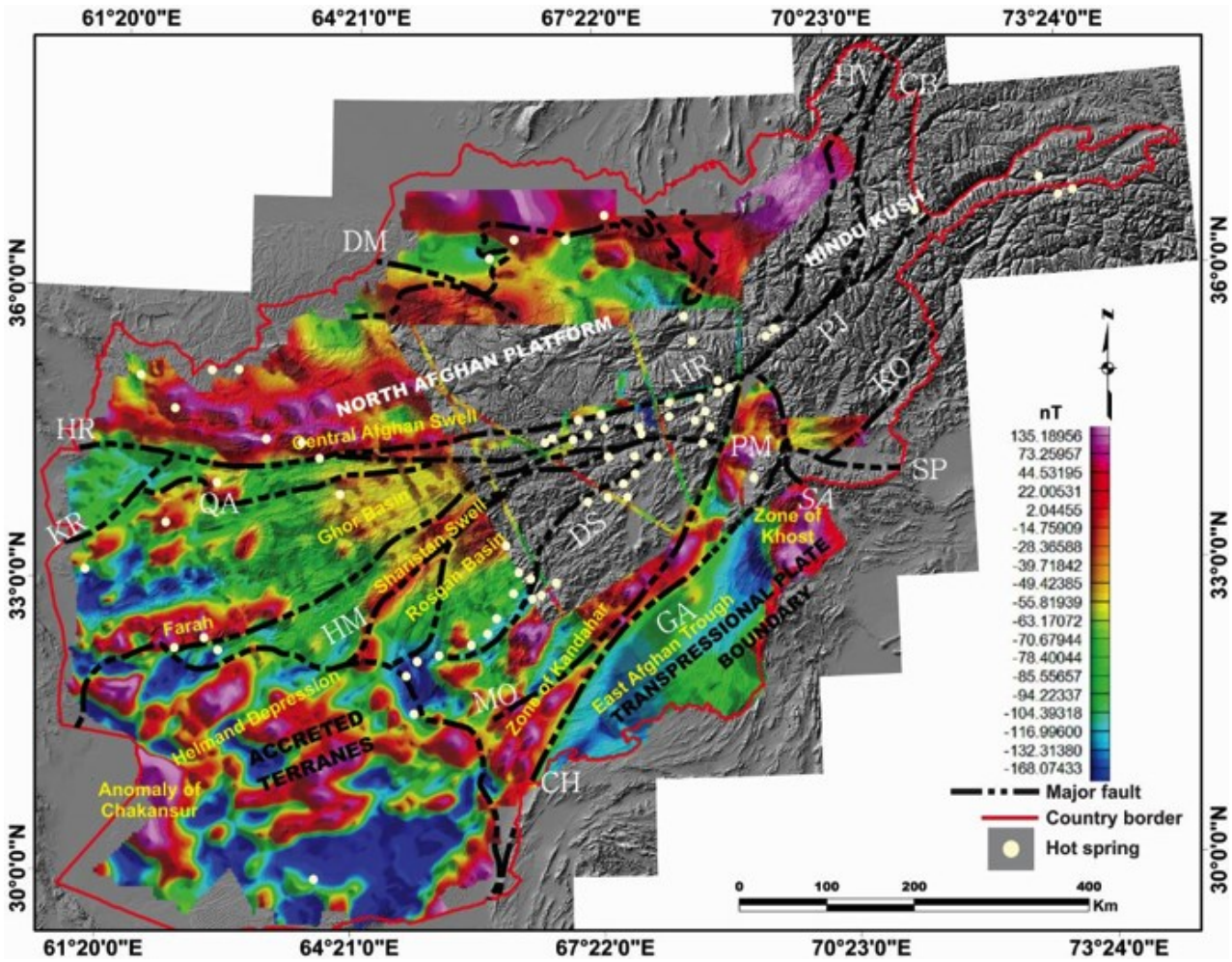

Figure 3: Reduced-to-pole magnetic map of Afghanistan, overlaid on the shaded relief (SRTM) map. The yellow text shows the major geological and morphological divisions related to the magnetic anomalies. White circles represent hot springs.

5. METHODOLOGY

To estimate the CPD we applied the method of spectral analysis to the observed aeromagnetic data in Afghanistan. Following the method presented by Tanaka et al. (1999), it was assumed that the layer extends infinitely in all horizontal directions. The depth to a magnetic source's upper bound is smaller than the magnetic source's horizontal scale, and that magnetization $\boldsymbol{M}(x, y)$ is a random function of x and y. Blakely (1995) introduced the power-density spectra of the total-field anomaly $\Phi_{\Delta T}$

$$\Phi_{\Delta T}(k_x, k_y) = \Phi_M(k_x, k_y) \times F(k_x, k_y) \tag{1a}$$

$$F(k_x, k_y) = 4\pi^2 C_m^2 |\Theta_m|^2 |\Theta_f|^2 e^{-2|k|Z_t}\left(1 - e^{-|k|(Z_b - Z_t)}\right)^2 \tag{1b}$$

Φ_M is the power-density spectra of the magnetization, C_m is a proportionality constant, Θ_m and Θ_f are factors for magnetization direction and geomagnetic field direction, and Z_t and Z_b are top and basal depth of magnetic source, respectively.

The above equation can be simplified by noting that all terms, except $|\Theta_m|^2$ and $|\Theta_f|^2$ are radially symmetric. Moreover, the radial average of Θ_m and Θ_f are constant. If $\boldsymbol{M}$ (x, y) is completely random and uncorrelated, Θ_m (k_x, k_y) is a constant. Hence, the radial average of $\Phi_{\Delta T}$ is:

$$\Phi_{\Delta T}(|k|) = Ae^{-2|k|Z_t}\left(1 - e^{-|k|(Z_b - Z_t)}\right)^2 \tag{2}$$

where A is a constant. For wavelengths less than about twice the thickness of the layer, Eq. (2) can be simplified as:

$$\ln\left[\Phi_{\Delta T}(|k|)^{1/2}\right] = \ln B - |k|Z_t \tag{3}$$

where B is a constant.

Okubo et al. (1985) proposed an algorithm to estimate the basal depth from magnetic data by considering a two-dimensional modeling technique for the determination of the depth to the base for a single block with the average parameters of the ensemble. Then, the algorithm estimates the depth to the centroid (Z_0) from the slope of radially averaged frequency-scaled power spectrum in the low wavenumber part and depth to the top (Z_t) from the slope of radially averaged power spectrum of magnetic anomaly.

From the slope of the power spectrum of total field anomaly, Z_t can be estimated.

Consequently, Eq. (2) can be-rewritten as:

$$\Phi_{\Delta T}(|k|)^{1/2} = \mathrm{C}e^{-|k|Z_0}\left(e^{-|k|(Z_t - Z_0)} - e^{-|k|(Z_b - Z_0)}\right) \tag{4}$$

where C is a constant. At long wavelength, Eq. (4) can be rewritten as:

$$\Phi_{\Delta T}(|k|)^{1/2} = \mathrm{C}e^{-|k|Z_0}\left(e^{-|k|(-\mathrm{d})} - e^{-|k|(\mathrm{d})}\right) \approx \mathrm{C}e^{-|k|Z_0}2|k|\mathrm{d} \tag{5}$$

where 2d is the thickness of the magnetic source. From Eq. (5), it can be concluded that:

$$\ln\left\{\left[\Phi_{\Delta T}(|k|)^{1/2}\right]/|k|\right\} = \ln \mathrm{D} - |k|Z_0 \tag{6}$$

where D is a constant.

By fitting a straight line through the high and low wavenumber parts from the radially averaged power spectrum of $\ln[\Phi_{\Delta T}(|\mathrm{k}|)^{1/2}]$ and $\ln[\Phi_{\Delta T}(|\mathrm{k}|)^{1/2}]/|\mathrm{k}|$, Z_t and Z_0 can be estimated. Finally, the basal depth of the magnetic source (Okubo et al., 1985; Tanaka et al., 1999) is:

$$Z_b = 2Z_0 - Z_t \tag{7}$$

The geothermal gradient (dT/dz) between the Earth's surface and the CPD (Z_b) can be defined by Eq. (8) (Tanaka et al., 1999; Stampolidis et al., 2005; Maden, 2010) and 580 °C is the Curie temperature for magnetite (Frost and Shive, 1986):

$$\frac{\mathrm{d}T}{\mathrm{d}Z} = \frac{580\ ^\circ\mathrm{C}}{Z_b} \tag{8}$$

Further, the geothermal gradient can be related to the heat flow q by using the formula (Turcotte and Schubert, 1982; Tanaka et al., 1999):

$$q = \lambda \frac{580\ ^\circ\mathrm{C}}{Z_b} \tag{9}$$

where λ is the coefficient of thermal conductivity. Eq. (9) demonstrates that the CPD is inversely proportional to the heat flow.

6. CURIE DEPTH AND HEAT FLOW ESTIMATES

In 2D magnetic maps, blocks (or windows) are used to calculate the radial power spectrum for each block and then estimate the CPD. Blakely (1988) applied a block size of 120 × 120 km to estimate the CPD in Nevada. Tanaka and Ishikawa (2005) and Manea and Manea (2011) used large blocks (~200 × 200 km) to map the Curie isotherm in Japan and Mexico, respectively. Trifonova et al. (2009) estimated the CPD in six blocks with dimensions 300 × 300 km for Bulgaria. Aboud et al. (2011) divided the magnetic data of Sinai Peninsula (Egypt) into nine overlapped subregions with a window size of 100 × 100 km. The depth resolution in such calculations is limited to the length of the aeromagnetic profile (L), the maximum CPD depth estimation is limited to 2π/L (Campos-Enriquez et al., 1990).

The study area extends from 30° to 35°30'N and from 61°30' to 66°30'E. The aeromagnetic data grid was divided into 15 blocks (A, B, C, D, ... , and O) having a size of 200 × 200 km. The choice of this block's dimensions is based on the criteria of minimal size of the block that does not cut the spectral peak (Ravat et al., 2007). To select the optimum window size for spectral analysis from each window, we reviewed previous studies by several authors (Blakely, 1995; Maus et al., 1997; Ravat et al., 2007). Blakely (1995) showed that the grid dimension should be five times Z_b. Ravat et al. (2007) suggested based on practical experience that the grid dimension should be no less than 200–300 km for an average Moho or Curie isotherm depth of roughly 30 km and preferably 10 times the depth to the bottom. Maus et al. (1997) recommended that the grid dimension should not be less than 1000 km.

In each block, both power spectrum and scaled-frequency power spectrum were calculated in order to estimate the depth to top (Z_t) and centroid (Z_0) depths of magnetic sources. From the relation of $Z_b = 2Z_0 - Z_t$, the curie depth point (Z_b) was computed, following the Okubo et al. (1985) procedure. The results are listed in Table 1.

The CPD (Z_b) map of central and western Afghanistan (Figure 4) shows that the depth are ranging from 16 km to 40 km. Shallow circular CPDs (less than 20 km) are identified at Helmand basin with its center at the boundary between accreted terranes and Afghan block. This boundary consists of deep-seated fault structure. This region coincides with the Kandahar arc. Shallow CPDs means high geothermal gradient (higher than 30 °C/km).

It is observed that a general increase of the CPD in all directions from this local shallow circular CPDs anomaly. Deep CPDs (20 to 40 km) are mainly observed toward the north of western Afghanistan, which may correspond to the subduction zone, where the Indian plate subducts beneath the Eurasian plate.

In Figure 5, two examples are shown of the averaged power spectrum of the aeromagnetic data from two sub-regions "N" and "O" with the magnetic source depth estimated based on linear segments of the energy decay curve. The calculated geothermal gradients (Figure 6) from Eq. (8) give values from 14.50 °C/km to 36.25 °C/km. Using Fourier's Law, estimations of heat-flow in the central and western parts of Afghanistan are performed on CPD estimates, the Curie-point for magnetite of 580 °C (Haggerty, 1978) and using an average thermal conductivity of λ=2.5 W/m°C (Stacey, 1977). The calculated heat-flow values range from 36.25 to 90 mW/m^2 (Figure 7).

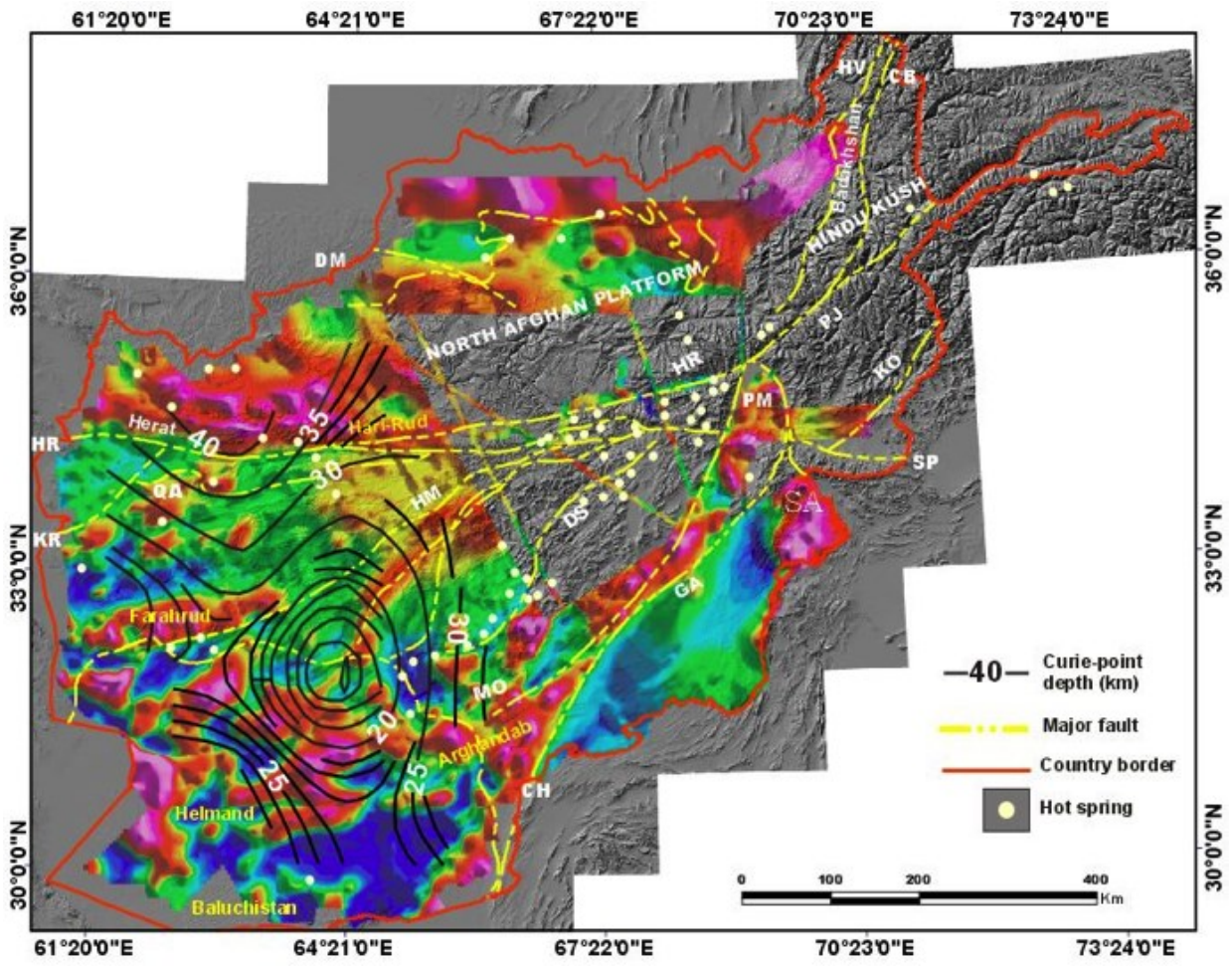

Figure 4: The CPD map of western Afghanistan and the main major faults in the region.

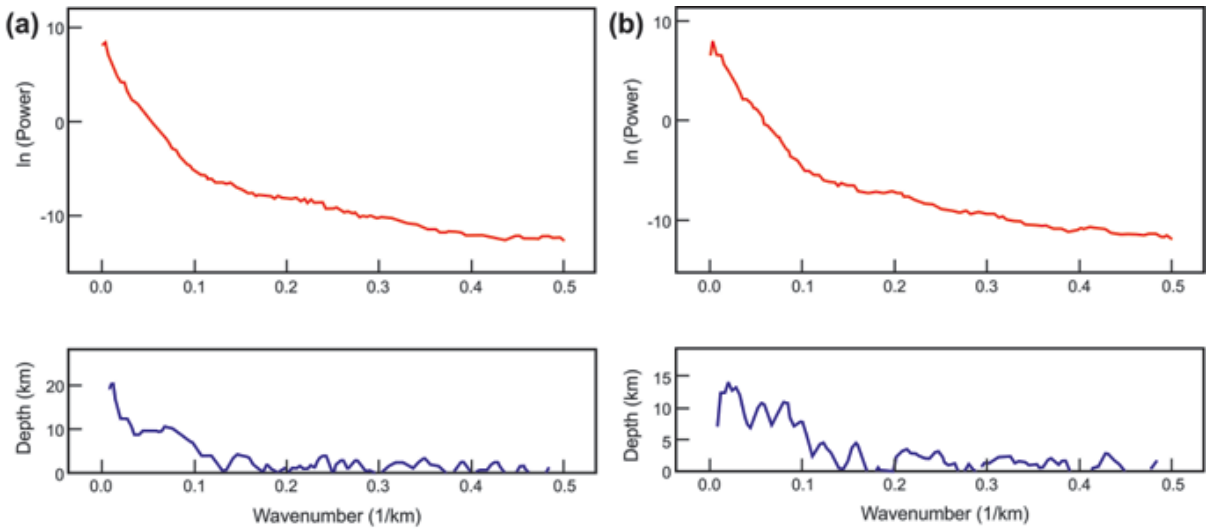

Figure 5: Radial power spectrum for two sub-regions "N" in (a) and "O" in (b), and their respective magnetic depths.

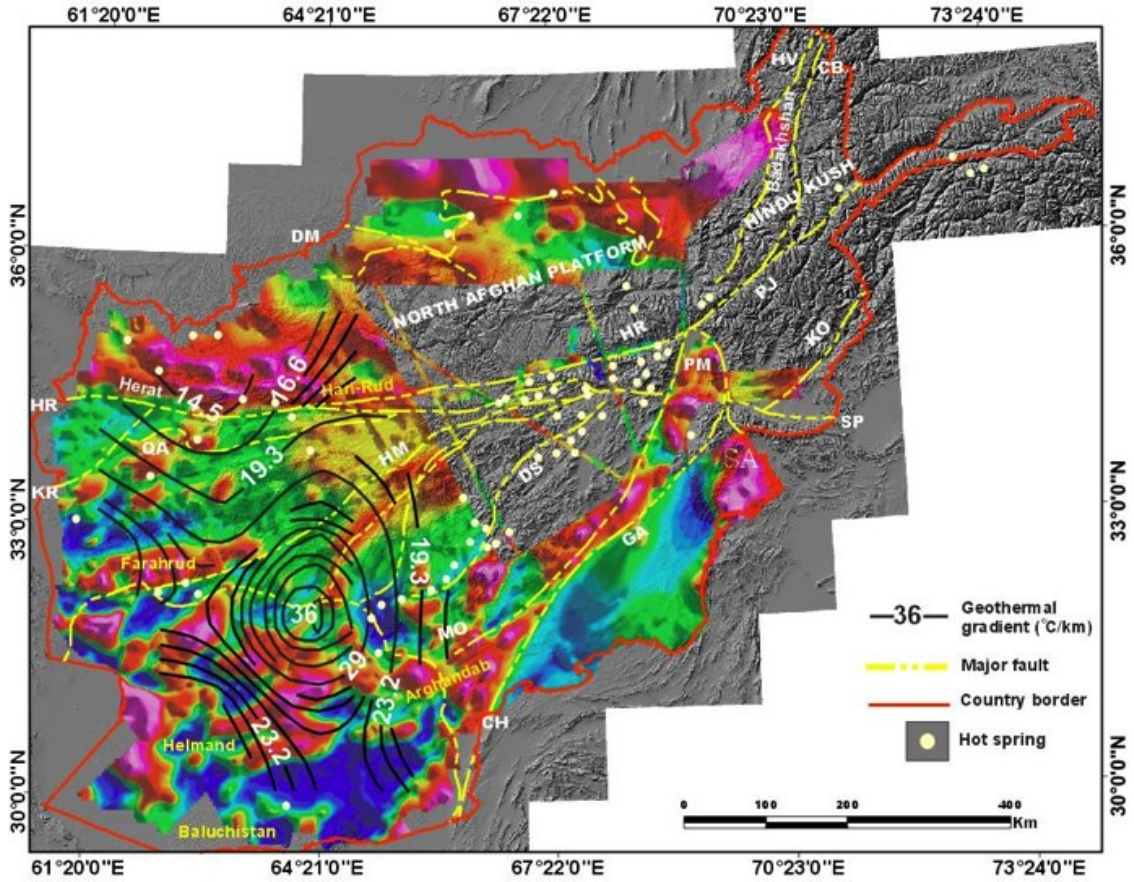

Figure 6: Geothermal gradient map of the study area.

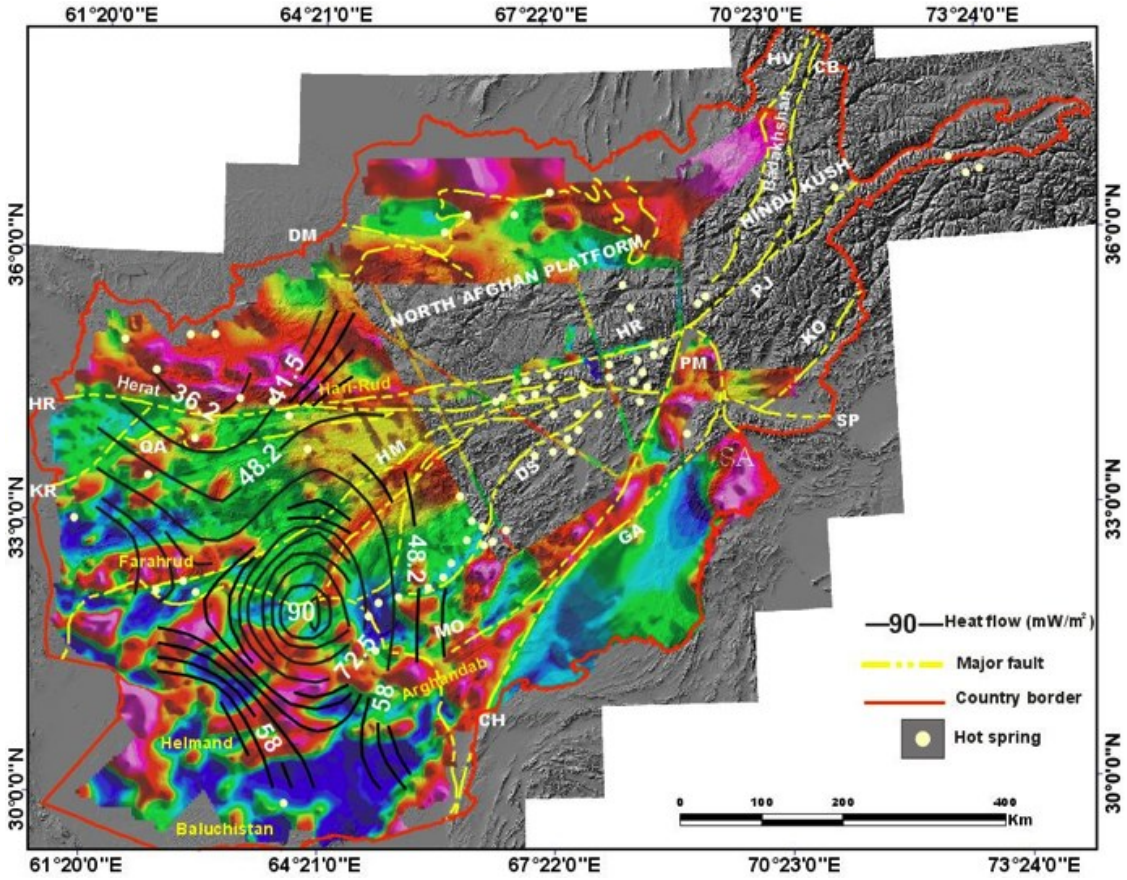

Figure 7: Heat flow map of the study area.

Table 1: Values of the top, centroid, and basal depths of the magnetic sources including error estimation for each parameter.

Sub-region	Z_t km (top depth)	Z_0 km (centroid depth)	Z_b=2Z_0-Z_t km (basal depth)
A	7.90	18.29	28.68
B	11.93	16.70	21.47
C	11.14	17.50	23.86
D	10.34	15.91	21.48
E	11.14	12.21	13.28
F	9.54	14.09	18.64
G	9.15	23.86	38.57
H	9.15	14.95	20.75
I	8.83	18.70	28.57
J	8.83	14.09	19.35
K	8.83	16.63	24.43
L	8.75	21.21	33.67
M	8.83	25.00	41.17
N	9.94	19.22	28.50
O	8.83	19.09	29.35

7. DISCUSSIONS AND CONCLUSIONS

In this study, the power spectral method is applied to aeromagnetic data from western Afghanistan with the aim of estimating depths to the Curie isotherm surface. In general, shallow CPDs can be associated with recent magmatic activity and thinned crust, whereas deep CPDs are related with thickened, cooled or old crust. In our case study, the deep CPD is related to the zone of the subduction slab of the Indian plate and the shallow CPDs are related to the Kandahar arc (Figure 8).

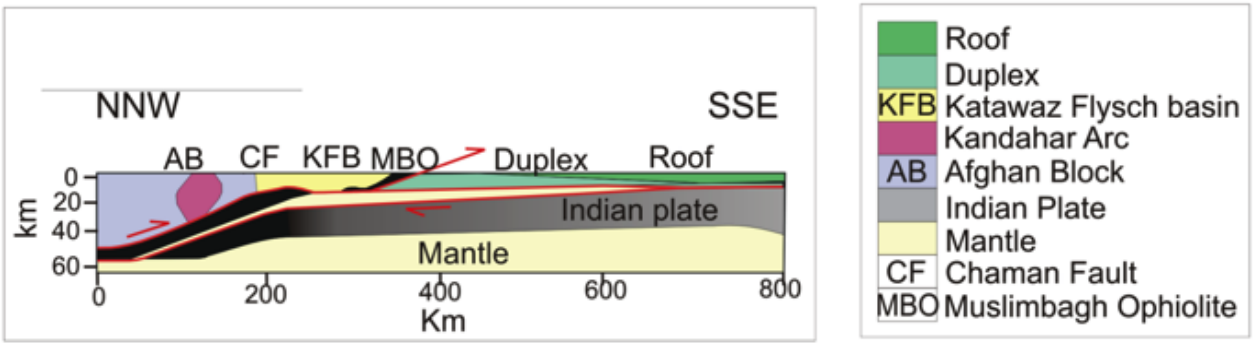

Figure 8: Oblique collision of northwestern margin of Indian subcontinent initiated by obduction of Muslimbagh ophiolites during Paleocene-Early Eocene. Khojak flysch is deposited on remaining oceanic lithosphere during Eocene-late Oligocene – early Himalayan uplift provides sediment source. Continued oblique convergence in late Oligocene-early Miocene (25 Ma) results in final closure of Tethys and initiation of sinistral strike-slip Chaman fault system. Since the Miocene, an estimated 353 ± 25 km of shortening has occurred in NW/SE sense (USGS, 2014).

In conclusion, the main findings of the current study can be summarized as follows:

- The estimated CPD from aeromagnetic data from western Afghanistan are ranging from 16 to 40 km. Deep CPD (30 – 40 km) area corresponds to the region where the Indian plate subducs beneath the Eurasian plate. The shallow CPDs could be explained by the upwelling of the Kandahar arc and are promising regions for future geothermal exploration.

- The calculated geothermal gradients from the relationship between CPD and Curie temperature (580 ˚C) give values from 14.50 °C/km to 36.25 °C/km.

- The heat flow values of western Afghanistan are ranging between 36.25 and 90 mW/m^2.

- The geothermal activity in western Afghanistan is mainly controlled by the deep-structures and faults generated from the active tectonic due to collision tectonics in this region.

REFERENCES

Aboud, E., Salem, A., Mekkawi, M.: Curie depth map for Sinai Peninsula, Egypt deduced from the analysis of magnetic data, *Tectonophysics*, **506**, (2011), 46–54.

Ashan, Said, Hussain, Sardar, Kohistany, A.H., Shenwary, G.S., Mutty, A.S., Daud, M.A., Abraham, J.D., Anderson, E.D., Drenth, B.J., Finn, C.A., Kucks, R.P., Lindsay, C.R., Phillips, J.D., Sweeney, R.E., Brozena, J.M., Ball, D.C., Childers, V.A., Gardner, J.M., Jarvis, J.L., Liang, R.T.: Aeromagnetic survey in Afghanistan: U.S. Geological Survey Open-File Report 2007-1247 (2007)

Aydin, I., Karat, H.I., and Kocak, A.: Curie-point depths map of Turkey, *Geophys. J. Int*., **162**, (2005), 633–640.

Belianin, V.I., Sobolev, B.I., and Ataei, G.: The Report of Studies on Mineral Waters of Afghanistan from 1969-1970. Geo. Surv. Afgh., Kabul (1970)

Bhattacharyya, B.K., and Leu, L.K.: Analysis of magnetic anomalies over Yellowstone National Park: mapping the Curie point depth isothermal surface for geothermal reconnaissance, *J. Geophys. Res*., **80**, (1975), 4461–4465.

Blakely, R.J.: Curie temperature isotherm analysis and tectonic implications of aeromagnetic data from Nevada, *J. Geophys. Res.*, **93** (B10), (1988), 11,817–11,832.

Blakely, R.J.: Potential Theory in Gravity and Magnetic Applications, Cambridge University Press, Cambridge, U. K. (1995)

Bosum, W., Hahn, A., Kind, E.G., Weippert, D.: Airborne magnetometer survey in the Kingdom of Afghanistan, Geological Survey of the Federal Republic of Germany, (1968), 46 p.

Bouligand, C., Glen, J.M.G., Blakely, R.J.: Mapping Curie temperature depth in the western United States with a fractal model for crustal magnetization, *Journal of Geophysical Research*, **114**, B11104, (2009), 1-25. DOI: 10.1029/2009JB006494

Campos-Enriquez, J.O., Arroyo-Esquivel, M.A., Urrutia-Fucugauchi, J.: Basement, curie isotherm and shallow crustal structure of the trans-Mexican volcanic belt, from aeromagnetic data, *Tectonophysics*, **172**, (1990), 77-90.

Chiozzi, P., Matsushima, J., Okubo, Y., Pasquale, V., Verdoya, M.: Curie-point depth from spectral analysis of magnetic data in central-southern Europe, *Physics of the Earth and Planetary Sciences*, **152**, (2005), 267-276.

De Ritis, R., Ravat, D., Ventura, G., Chiappini, M.: Curie isotherm depth from aeromagnetic data constraining shallow heat source depths in the central Aeolian Ridge (Southern Tyrrhenian Sea, Italy), *Bull. Volcanol.*, **75** (710), (2013), 11 pp.

Ebbing, J., Gernigon, L., Pascal, C., Olesen, O., Osmundsen, P. T.: A discussion of structural and thermal control of magnetic anomalies on the mid-Norwegian margin, *Geophysical Prospecting*, **57**, (2009), 665-681.

Espinosa-Cardeña, J.M., Campos-Enriquez, J.O.: Curie point depth from spectral analysis of aeromagnetic data from Cerro Prieto geothermal area, Baja California, Mexico, *Journal of Volcanology and Geothermal Research*, **176**, (2008), 601-609.

Frost, B.R., Shive, P.N.: Magnetic mineralogy of the lower continental crus, *J. Geophys. Res.*, **91**, (1986), 6513–6521.

Guimarães, S.N.P., Ravat, D., Hamza, V.M.: Combined use of the centroid and matched filtering spectral magnetic methods in determining thermomagnetic characteristics of the crust in the structural provinces of Central Brazil, *Tectonophysics*, (2014) in press. http://dx.doi.org/10.1016/j.tecto.2014.01.025

Haggerty, S.E.: Mineralogical constraints on Curie isotherm in deep crustal magnetic anomalies, *Geophy. Res. Lett.*, **5** (2), (1978), 105-109.

Hinze, W.J., von Frese R.R.B., Saad, A.H.: Gravity and magnetic exploration, Cambridge University Press, (2013), 512 p.

Hsieh, H.H., Chen, C.H., Lin, PY., Yen, H.Y.: Curie point depth from spectral analysis of magnetic data in Taiwan, *Journal of Asian Earth Sciences*, **90**, (2014), 26-33. http://dx.doi.org/10.1016/j.jseaes.2014.04.007

Karastathis, V.K., Papoulia, J., Di Fiore, B., Makris, J., Tsambas, A., Stampolidis, A., Papadopoulos, G.A.: Deep structure investigations of the geothermal field of the North Euboean Gulf, Greece, using 3-D local earthquake tomography and Curie Point Depth analysis, *Journal of Volcanology and Geothermal Research*, **206**, (2011), 106-120.

Kurenoe, V.V., and Belianin, V.I.: Mineral waters of Afghanistan, Dept. Geol. Surv., Kabul, Afghanistan (1969)

Maden, N.: Curie-point depth from spectral analysis of magnetic data in Erciyes stratovolcano (central Turkey), *Pure and Applied Geophysics*, **167**, (2010), 349-358.

Manea, M., Manea, V.C., 2011. Curie point depth estimates and correlation with subduction in Mexico, *Pure and Applied Geophysics*, **168** (8-9), (2011), 1489-1499. DOI 10.1007/s00024-010-0238-2

Maus, S., Gordon, D., and Faihead, J.D.: Curie-temperature depth estimation using a self-similar magnetization model, *Geophys. J. Int.*, **129**, (1997), 163-168.

Mihalasky M.J., Doebrich, J.L., Wahl, R.W., Ludington, S.D., Orris, G.J., Bliss, J.D., Sutphin, D.M., Schruben, P.G., Bolm, K.S., Hubbard, B.E., Mars, J.C., Peters, S.G., Wandrey, C.J., Chirico, Pete: Geographic information system (GIS) to accompany the non-fuel mineral resource assessment of Afghanistan, appendix 1 in Peters, S.G.,. Ludington, S.D., Orris, G.J., Sutphin, D.M., Bliss, J.D., and Rytuba J.J., eds., and the U.S. Geological Survey-Afghanistan Ministry of Mines Joint Mineral Resource Assessment Team, Preliminary Non-Fuel Mineral Resource Assessment of Afghanistan: U.S. Geological Survey Open-File Report, 2007-1214 (version 1), two discs (2007)

Musazai, A.: Research on ultrabasites of Afghanistan and their industrial mineralization. Research monograph, Kabul Polytechnic Inst., Afghanistan, (1994), 127pp. (in Persian)

Okubo, Y. and Matsunaga, T.: Curie point depth in northeast Japan and its correlation with regional thermal structure and seismicity, *Journal of Geophysical Research*, **99**, (1994). doi: 10.1029/94JB01336. issn: 0148-0227.

Okubo, Y., Graf, R.J., Hansen, R.O., Ogowa, K., and Tsu, H.: Curie point depth of the island of Kyushu and surrounding areas, Japan, *Geophysics*, **50**, (1985), 481–494.

Rajaram, M., Anand, S.P., Hemant, K., Purucker, M.E.: Curie isotherm map of Indian subcontinent from satellite and aeromagnetic data, *Earth and Planetary Science Letters*, **281**, 3-4, (2009), 147-158.

Ravat, D., Pignatelli, A., Nicolosi, I., Chiappini, M.: A study of spectral methods of estimating the depth to the bottom of magnetic sources from near-surface magnetic anomaly data, *Geophys. J. Int.*, **169**, (2007), 421-434.

Ross, H.E., Blakely, R.J., and Zoback, M.D.: Testing the use of aeromagnetic data for the determination of Curie depth in California, *Geophysics*, **71** (5), (2006), L51–L59. doi:10.1190/ 1.2335572.

Rozimant, K., Buyuksarac, A., Bektas, O.: Interpretation of Magnetic Anomalies and estimation of depth of magnetic crust in Slovakia, *Pure. Appl. Geophys.*, **166**, (2009), 471–484.

Ruiz, F., and Introcaso, A.: Curie Point Depths beneath Precordillera Cuyana and Sierras Pampeanas obtained from spectral analysis of magnetic anomalies, *Gondwana Research*, **7** (4), (2004), 1133–1142.

Saba, D.S., Najaf, M.E., Musazai, A.M., Taraki, S.A.: Geothermal energy in Afghanistan: prospects and potential. Accessed on May 2014 at http://www.mindfully.org/Energy/2004/Afghanistan-Geothermal-Energy1feb04.htm (2004)

Salem, A., Green, C., Ravat, D., Singh, K.H., East, P., Fairhead, D., Mogren, S., Biegert, E.: Depth to Curie temperature across the central Red Sea from magnetic data using the de-fractal method, *Tectonophysics*, (2014). In press. http://dx.doi.org/10.1016/j.tecto.2014.04.027

Shareq, A., Chemeriov, V.M., and Dronov, V.I.: Geology and Mineral Resources of Afghanistan, Book II: Geology. Nedra, Moscow, 535 pp. (in Russian) (1980)

Shenwary, G.S., Kohistany, A.H., Hussain, Sardar, Ashan, Said, Mutty, A.S., Daud, M.A., Wussow, M.D., Sweeney, R.E., Phillips, J.D., Lindsay, C.R., Kucks, R.P., Finn, C.A., Drenth, B.J., Anderson, E.D., Abraham, J.D., Liang, R.T., Jarvis, J.L., Gardner, J.M., Childers, V.A., Ball, D.C., Brozena, J.M.: Aeromagnetic surveys in Afghanistan: an updated website for distribution of data: U.S. Geological Survey Open-File Report 2011–1055, (2011), 8 p.

Stacey, F.D.: Physics of the Earth, 2nd Edition, Wiley, New York, (1977), 414 pp.

Stampolidis, A., Kane, I., Tsokas, G.N., Tsourlos, P.: Curie point depths of Albania inferred from ground total field magnetic data, *Surveys in Geophysics*, **26**, (2005), 461-480.

Tanaka, A., and Ishikawa, Y.: Crustal thermal regime inferred from magnetic anomaly data and its relationship to seismogenic layer thickness: the Japanese islands case study, *Physics of the Earth and Planetary Interiors*, **152**, (2005), 257–266.

Tanaka, A., Okubo, Y., Matsubayashi, O.: Curie point depth based on spectrum analysis of the magnetic anomaly data in East and Southeast Asia, *Tectonophysics*, **306**, (1999), 461–470.

Tapponnier, M., Mattauer, M., Proust, F., Cassaigneau, C.: Mesozoic ophiolites, sutures, and large-scale tectonic movements in Afghanistan, *Earth Planet. Sci. Lett.*, **52**, (1981), 355–371.

Trifonova, P., Zhalev, Zh., Petrova, T., Bojadgieva, K.: Curie point depths of Bulgarian territory inferred from geomagnetic observations and its correlation with regional thermal structure and seismicity, *Tectonophysics*, **473**, (2009), 362-374.

Turcotte, D.L., Schubert, G.: Geodynamics, Cambridge University Press, New York (1982)

USGS: Modern Concepts in Earth Science. Accessed on May 2014 at escweb.wr.usgs.gov

Wasilewski, P.J., Thomas, H.H., Mayhew, M.A.: The Moho as a magnetic boundary, *Geophysical Research Letters*, **6** (7), (1979), 541-544.